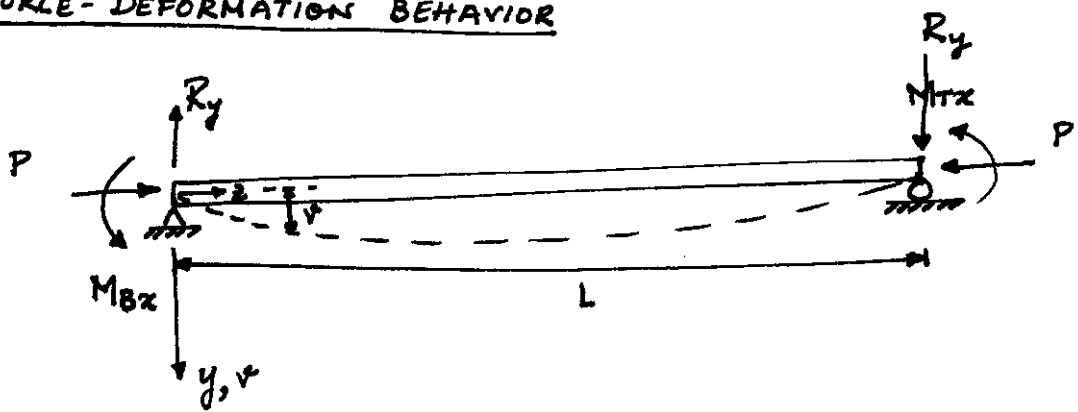


### 4 Beam-Columns

- Members subjected to bending & axial compression are called beam-columns.
- Beam-Columns in frames are usually subjected to end forces only. However, beam-columns may also be subjected to transverse forces in addition to end-forces.
- Behavior of beam-columns is similar somewhat to beams & columns.

#### 4.1 FORCE-DEFORMATION BEHAVIOR



Let,

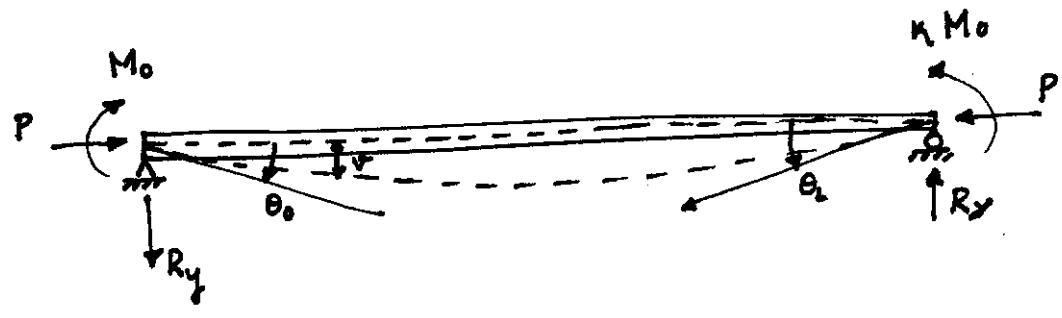
$$M_0 = -M_{Bz}$$

$$\kappa M_0 = M_{Tz}$$

} change of variable

$$-1 \leq \kappa \leq 1$$

$\int_0^L$ 
 $\left. \begin{array}{l} \kappa = 1 \rightarrow \\ \kappa = -1 \rightarrow \end{array} \right\}$



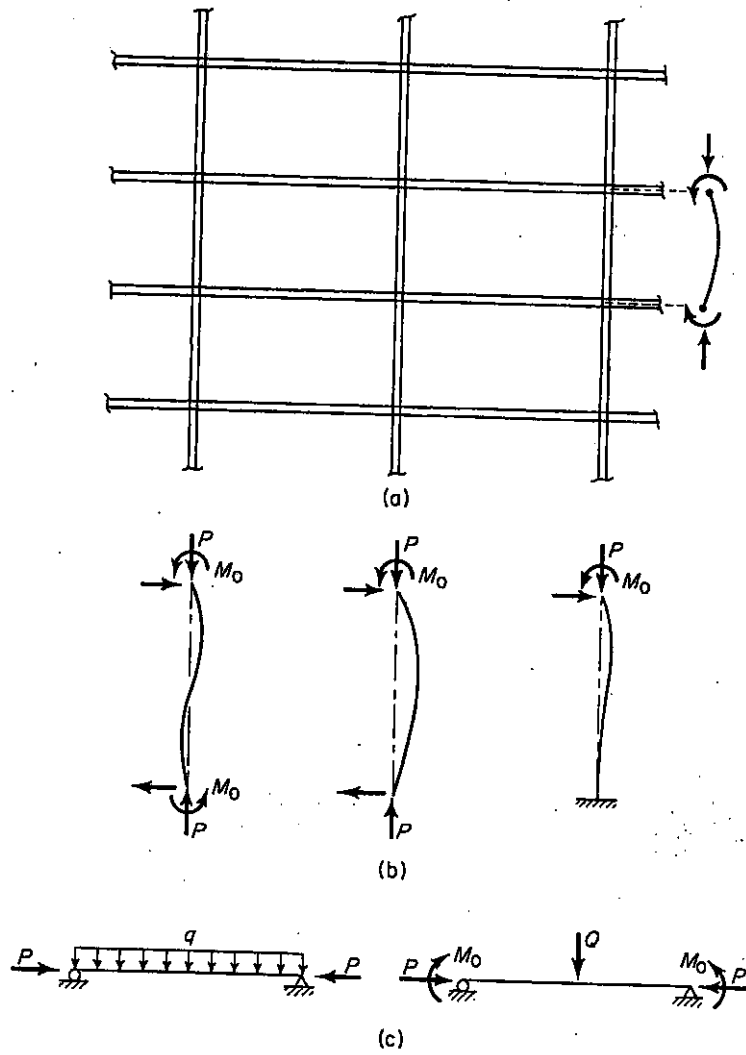


Fig. 5.1. Beam-columns and beam-column loadings. (a) Beam-columns in a frame, (b) typical beam-columns in frames, (c) typical beam-columns with transverse loads.

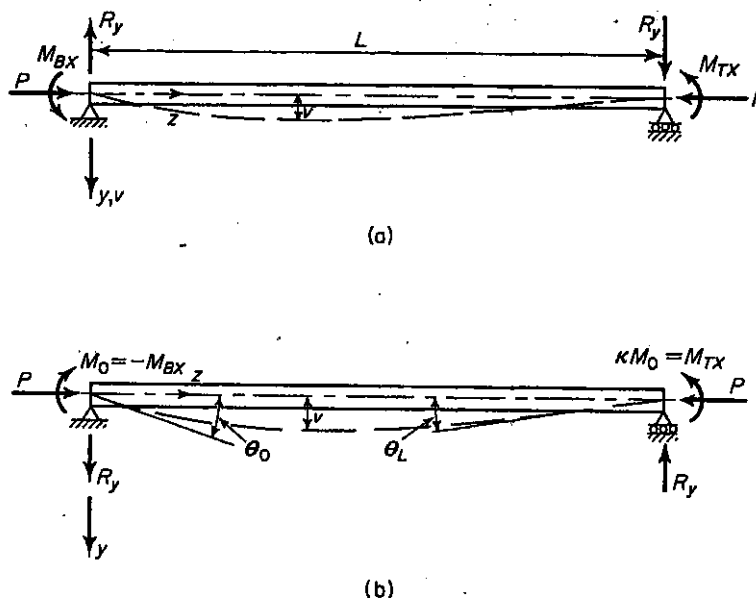
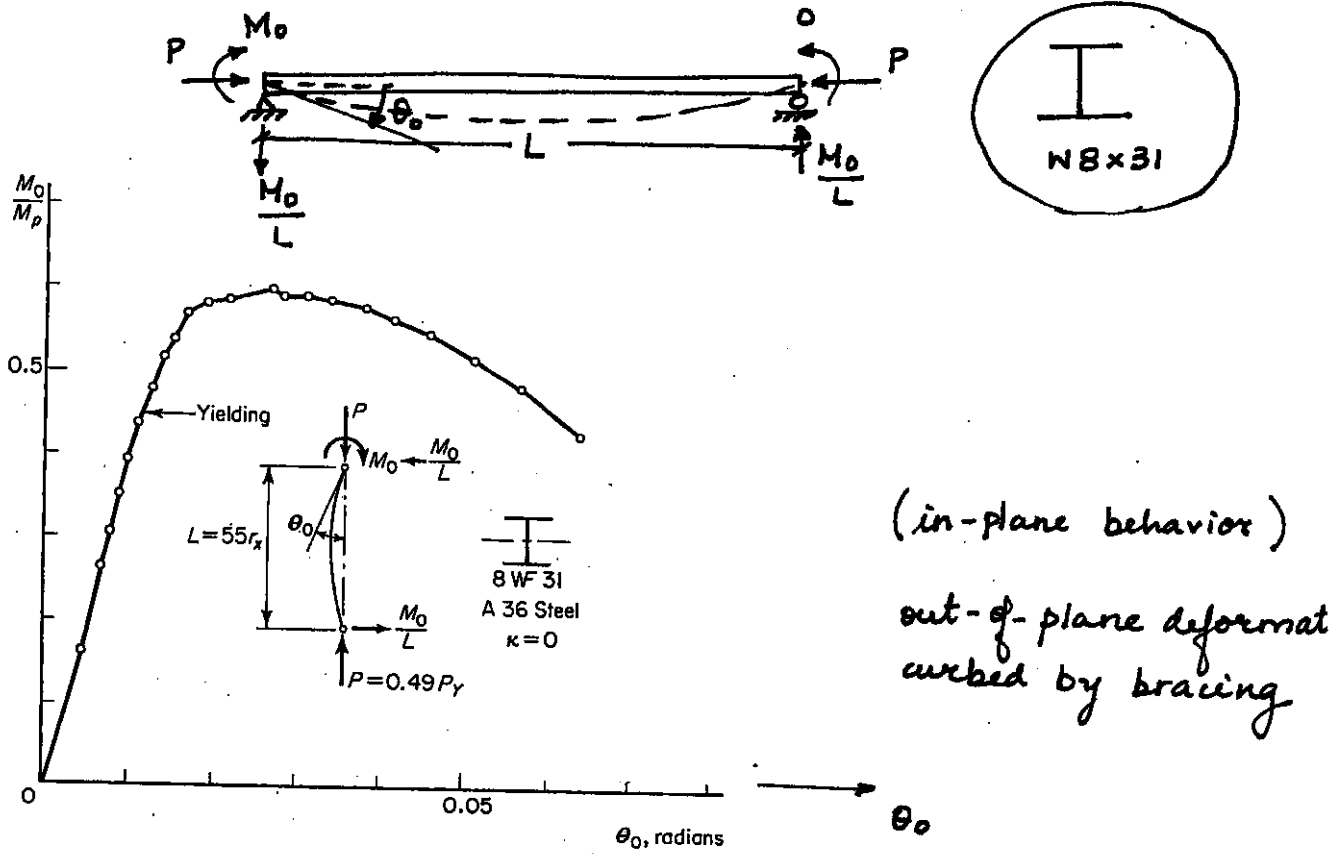


Fig. 5.2. End forces, dimensions, and sign conventions. (a) Beam-columns with end forces, (b) beam-column sign conventions.

- Consider, the experimental behavior of a wide-flange beam-column subjected to  $P = 0.49 P_y$  (concentric) &  $M_0$  (increasing) with  $\kappa = 0$



(in-plane behavior)  
 out-of-plane deformation  
 curved by bracing

- Behavior of beam-columns is different than the behavior of beams or columns

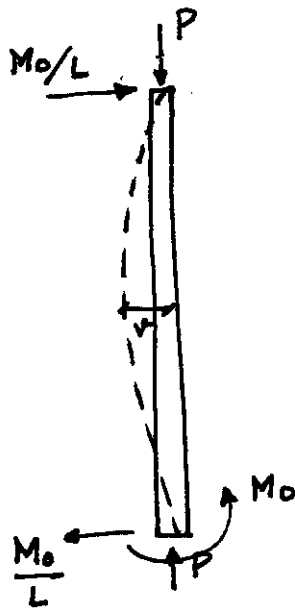
$P < P_{max}/column \rightarrow$  Therefore, some reserve capacity to carry  $M$

$M < M_p \rightarrow$  moment carried is less than  $M_p$  because  $P \neq 0$

&  $M_0|_{max}$  for the beam-column is not maintained through indefinite rotation.

- Note that for beams moment is reduced due to LTB or LB buckling. → out-of-plane

But, for the beam-column →  $M_o / \max$  is reached due to in-plane behavior only → no LTB or LB before  $M_o / \max$  is reached



$$M(z) = M_o \left(1 - \frac{z}{L}\right) + P v$$

secondary moment

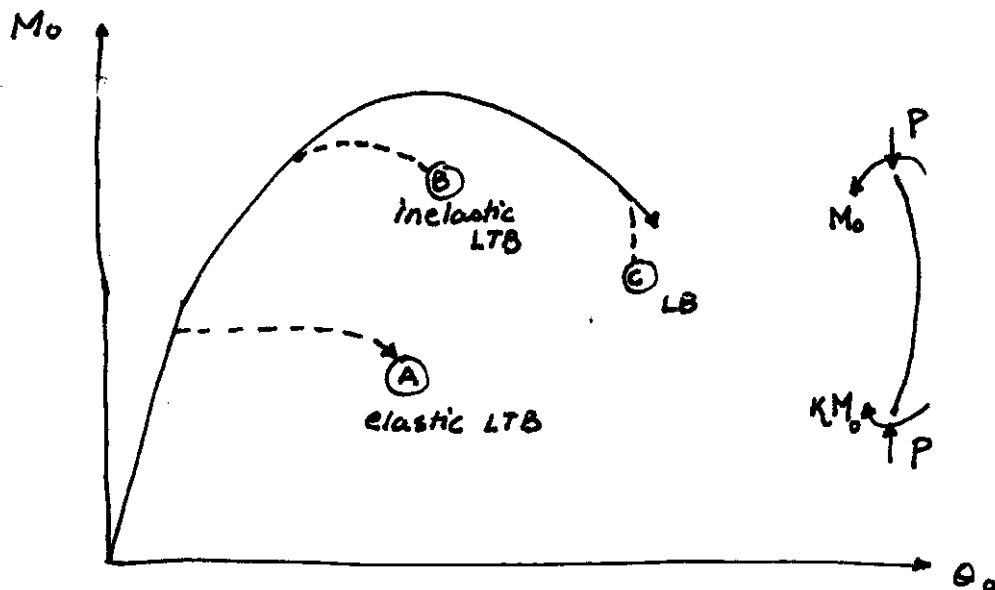
As  $M_o$  increases,  $v$  increases

↓  
increasing  $Pv$

When member yields,  $v$  increases more rapidly

↓  
 $Pv$  increases at such a rate that it dominates

- Consider, overall behavior



$P$  &  $K$  are constant

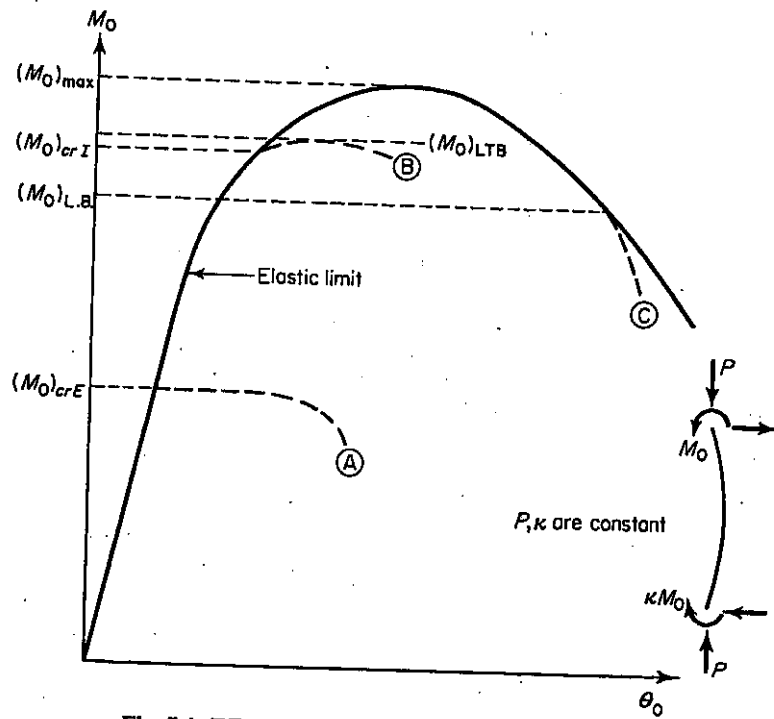


Fig. 5.4. Effect of lateral-torsional and local buckling

4.2 Elastic BEHAVIOR

$$M_{By} = M_{Ty} = 0, \quad M_{Bx} = -M_0 \quad \& \quad M_{Tx} = \kappa M_0, \quad P = P$$

- ∴ 2<sup>nd</sup> order differential equations are:

$$EI_x v'' + Pv - P\alpha_0 \phi = M_0 \left[ -1 + \frac{z}{L} (1-\kappa) \right] \longrightarrow (1)$$

$$EI_y u'' + Pu + M_0 \phi \left[ 1 - \frac{z}{L} (1-\kappa) \right] + Py_0 \phi = 0 \longrightarrow (2)$$

$$EI_\omega \phi''' - (GK_T + \bar{K}) \phi' + M_0 u' \left[ 1 - \frac{z}{L} (1-\kappa) \right] + Py_0 u' - P\alpha_0 v' + \frac{M_0}{L} (1-\kappa) u = 0 \longrightarrow (3)$$

- Eq. (1), (2) & (3) are coupled. Eq. (1) is also coupled through

This means that for most general cross-sections with  $\alpha_0 \neq 0$  &  $y_0 \neq 0 \rightarrow$  applying  $P$  &  $M_0 \rightarrow u, v, \& \phi$

- For a singly symmetric cross-section with  $\alpha_0 = 0$  & moments acting in the plane of symmetry ( $y-z$  plane)

$$EI_x v'' + Pv = M_0 \left( -1 + \frac{z}{L} (1-\kappa) \right) \longrightarrow (4)$$

$$EI_y u'' + Pu + M_0 \phi \left[ 1 - \frac{z}{L} (1-\kappa) \right] + Py_0 \phi = 0 \longrightarrow (5)$$

$$EI_\omega \phi''' - (GK_T + \bar{K}) \phi' + M_0 u' \left[ 1 - \frac{z}{L} (1-\kappa) \right] + Py_0 u' - \cancel{P\alpha_0 v'} + \frac{M_0}{L} (1-\kappa) u = 0 \longrightarrow (6)$$

∴ differentiating these equations

$$(7) \quad EI_x v^{iv} + P v'' = 0$$

$$(8) \quad EI_y u^{iv} + P u'' + M_0 \left[ 1 - \frac{z}{L} (1-\kappa) \right] \phi'' - \frac{2 M_0}{L} (1-\kappa) \phi' + P_{y_0} \phi'' = 0$$

$$(9) \quad EI_\omega \phi^{iv} - (G K_T + \bar{K}) \phi'' - \bar{K}' \phi' + M_0 \left[ 1 - \frac{z}{L} (1-\kappa) \right] u'' + P_{y_0} u'' = 0$$

The value of  $\bar{K} = \int_A \sigma a^2 dA$   $\left. \vphantom{\int_A \sigma a^2 dA} \right\} \sigma = -\frac{P}{A} + \frac{M_x z}{I_x}$

$$(10) \quad \therefore \bar{K} = -P \bar{r}_0^2 + M_x \beta_x$$

$\swarrow$  column                       $\searrow$  beam

where,  $M_x = M_0 \left( 1 - \frac{z}{L} (1-\kappa) \right)$   $\rightarrow$  moment within the span of b.c.

∴ Eq. (9) can be written as

$$EI_\omega \phi^{iv} - \left[ G K_T - P \bar{r}_0^2 + M_x \beta_x \right] \phi'' + M_0 \beta_x \phi' \frac{(1-\kappa)}{L} + M_x u'' + P_{y_0} u'' = 0 \quad \rightarrow (11)$$

- Now the final equations are (7), (8) & (11)  
 where, Eq. (7) is uncoupled from eq. (8) & (11)

Eq. (7) defines the in-plane bending deformations

Eq. (8) & (11) correspond to the occurrence of LTB.

## 4.2.1 IN-PLANE behavior &amp; strength

$$\therefore EI_x v^{iv} + P v'' = 0$$

$$\therefore v^{iv} + \frac{P}{EI_x} v'' = 0$$

$$\text{Let } \frac{P}{EI_x} = F_v^2$$

$$\therefore v^{iv} + F_v^2 v'' = 0 \quad \longrightarrow \quad (12)$$

$$\text{Solution is: } v = C_1 \sin(F_v z) + C_2 \cos(F_v z) + C_3 z + C_4 \quad \longrightarrow \quad (13)$$

$$\text{Use boundary conditions: } v(0) = v(L) = 0$$

$$v''(0) = -\frac{M_0}{EI_x} \quad \& \quad v''(L) = -\frac{\kappa M_0}{EI_x}$$

solve for constants of integrations:

$$(14) \quad \therefore v = \frac{M_0}{P} \left[ \left( \frac{\kappa - \cos F_v L}{\sin F_v L} \right) \sin F_v z + \cos F_v z + \frac{z}{L} (1 - \kappa) - 1 \right]$$

$\therefore$  bending moment at any point  $z$  is computed as:

$$(15) \quad M = -EI_x v'' = M_0 \left[ \left( \frac{\kappa - \cos F_v L}{\sin F_v L} \right) \sin(F_v z) + \cos(F_v z) \right]$$

max. moment location & value

$$\frac{dM}{dz} = 0 \quad \therefore M_0 \left[ \left( \frac{\kappa - \cos F_v L}{\sin F_v L} \right) \cos(F_v z) - \sin(F_v z) \right] = 0$$



∴ Max. moment occurs when

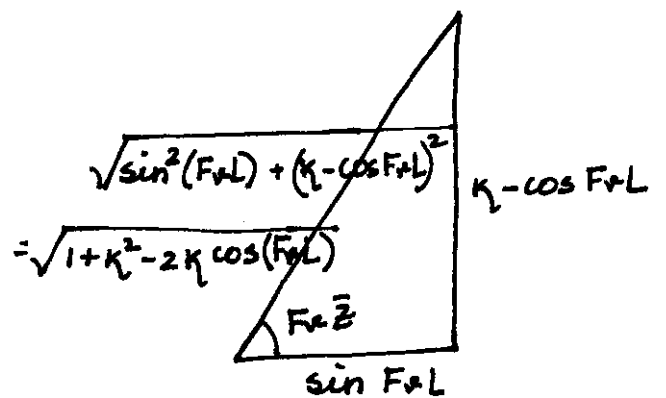
$$\tan(F\bar{z}) = \frac{\kappa - \cos F\bar{z}}{\sin F\bar{z}} \longrightarrow (16)$$

corresponding  $M_{max} = M_0 \left[ \tan(F\bar{z}) \sin(F\bar{z}) + \cos(F\bar{z}) \right]$

which can be simplified to  $M_{max} = M_0 \varphi \longrightarrow (17)$

where,  $\varphi = \frac{1}{\cos(F\bar{z})}$

$$\therefore \varphi = \frac{\sqrt{1 + \kappa^2 - 2\kappa \cos(F\bar{z})}}{\sin(F\bar{z})}$$

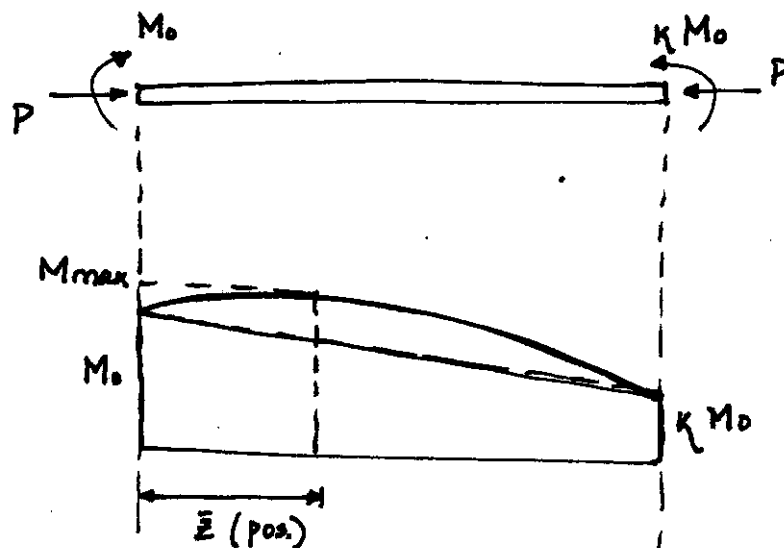


$$= \frac{\sqrt{1 + \kappa^2 - 2\kappa \cos(F\bar{z})}}{\sin(F\bar{z})}$$

$$\therefore M_{max} = \frac{M_0 \times \sqrt{1 + \kappa^2 - 2\kappa \cos(F\bar{z})}}{\sin(F\bar{z})} \longrightarrow (18)$$

• Thus, for a beam-column subjected to  $P$  &  $M$

Moment magnification



Location  $\bar{z}$  from :  $\cos (F\bar{z}) = \frac{\sin F+L}{\sqrt{1+k^2-2k \cos (F+L)}} \rightarrow (19)$

Eq. (19) may result in values of  $\bar{z}$  that are negative

- This means that  $M_{max}$  does not occur in  $0 \leq z \leq L$  and  $M_0$  is the max. moment for the beam-column

- ~~When~~ When does  $M_{max}$  occur within the span

If  $k \geq \cos (F+L) \rightarrow$  then  $\varphi = 1.0$  ( $M_{max}$  out span)

If  $k \leq \cos (F+L) \rightarrow$  then  $\varphi = \text{Eq. (18)}$  [ $M_{max}$  in span]

Another limiting situation, when  $P = P_{cr} = \frac{\pi^2 E I_x}{L^2}$

then, no moment can be applied

$\therefore M_0 = \frac{M_{max}}{\varphi} = 0$

$\therefore \varphi = \infty$

$\therefore \sin (F+L) = 0$

$\therefore (F+L)_{max} = \pi \rightarrow (20)$

## 4.2.2. IN-PLANE STRENGTH

Limit of applicability of the equations is when  $\sigma_Y$  is the max. stress

$$\therefore \sigma_{\max} = \sigma_Y = \frac{P}{A} + \frac{M_{\max}}{S_x} \quad \leftarrow \text{limiting condition}$$

$$\therefore \frac{P}{A \sigma_Y} + \frac{M_{\max}}{S_x \sigma_Y} = 1.0$$

$$\therefore \frac{P}{P_Y} + \frac{M_{\max}}{M_Y} = 1.0$$

$$\therefore \frac{P}{P_Y} + \varphi \frac{M_0}{M_Y} = 1.0$$

$\leftarrow$  Re expressed limiting condition  
 $\rightarrow$  (21)

$\swarrow$   
 amplification factor.

- Eq. (21) is also called an interaction equation

Thus for a given  $P$ , one can determine  $M_0$  for the beam-column to limit  $\sigma$  to  $\sigma_Y$ .

- Eq. (21) applies for  $0 \leq F+L \leq \pi$

$$\text{i.e. } 0 \leq L \sqrt{\frac{P}{EI_x}} \leq \pi$$

• In Eq. (21)

$$\text{If } \kappa \geq \cos(FvL) \text{ then } \varphi = \frac{\sqrt{1 + \kappa^2 - 2\kappa \cos(FvL)}}{\sin(FvL)}$$

$$\text{If } \kappa \leq \cos(FvL) \text{ then } \varphi = 1.0$$

• Plot relationship between  $\varphi$  &  $FvL$  for diff.  $\kappa$

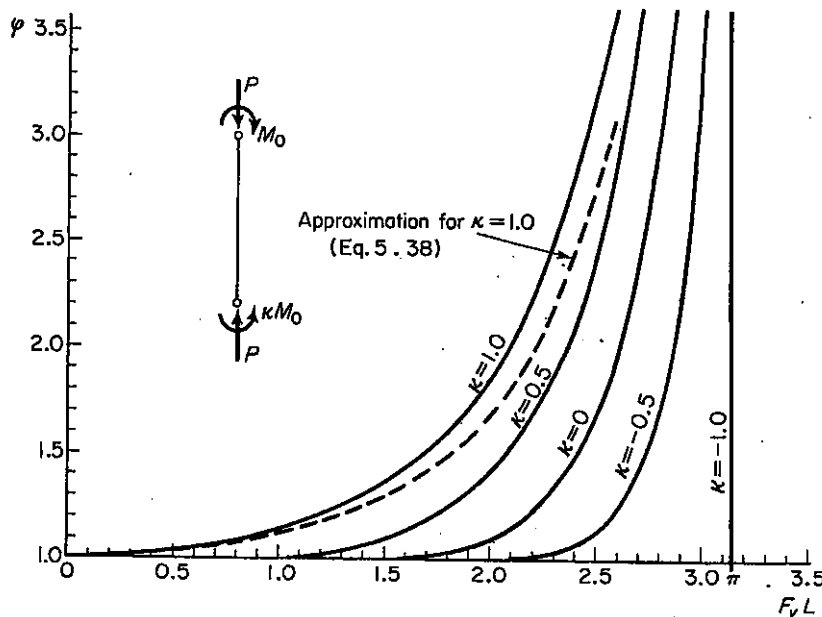


Fig. 5.7. Charts for determining  $\varphi$

$$\frac{P}{P_Y} + \varphi \frac{M_0}{M_Y} = 1.0 \quad \longrightarrow \quad \text{Eq. (2)}$$

$$\varphi \longrightarrow f(\kappa, F_{\nu}L)$$

$$\& \quad F_{\nu}L = L \sqrt{\frac{P}{EI_x}} = \pi \sqrt{\frac{P \times L^2}{\pi^2 EI_x}} = \pi \sqrt{\frac{P}{P_E}}$$

$$\therefore F_{\nu}L = \frac{L}{r_x} \sqrt{\frac{\sigma_y}{E} \times \frac{P}{P_Y}}$$

$\therefore$  The elastic in-plane strength depends on four non-dimensionalized parameters  $\frac{P}{P_Y}$ ,  $\frac{M_0}{M_Y}$ ,  $\eta$  &  $\frac{L}{r_x} \sqrt{E_y}$

• Interaction curves: Slenderness effects  $\left(\frac{L}{r_x}\right)$

$\frac{P}{P_Y} - \frac{M_0}{M_Y}$  interaction curves.

- Consider the effect of slenderness  $\frac{L}{r_x} \times \sqrt{E_y}$  for beam-columns bent into single curvature by equal end moments ( $\kappa = 1.0$ ).

- slender columns deflect more  $\rightarrow \therefore$  more  $P_{\nu}$  effects

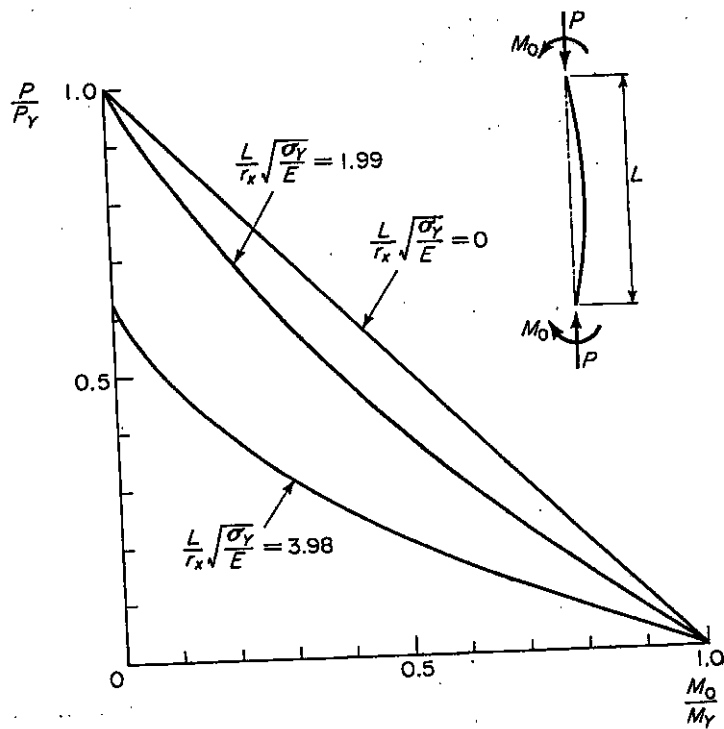


Fig. 5.8. Elastic limit interaction curves for  $\kappa = 1.0$

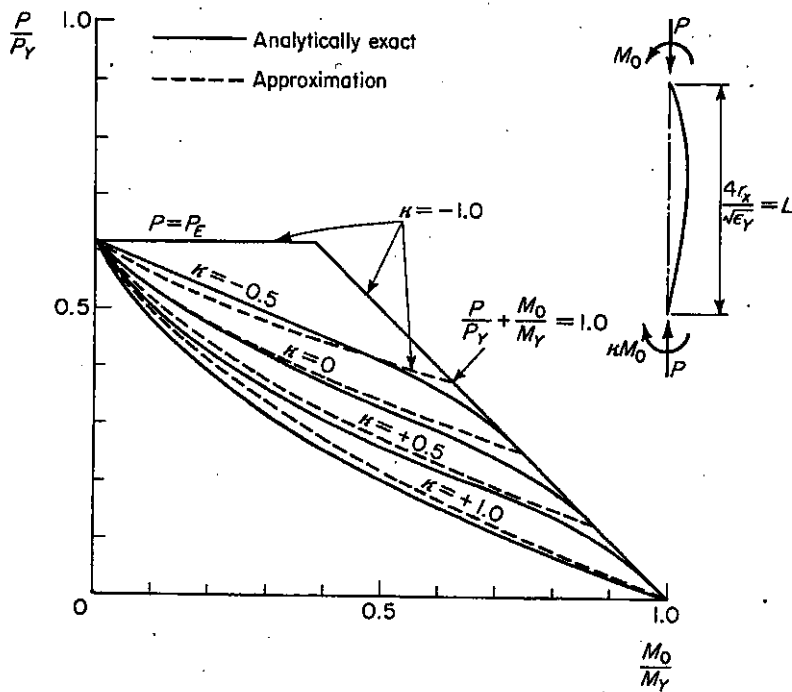


Fig. 5.9. Exact and approximate elastic-limit interaction curves

- Inter equation : effect of moment gradient  $\kappa$ 
  - $\frac{L}{r_x} \times \sqrt{E_y} = 4.0$  single curvature  $\kappa = 1.0$
  - double curvature  $\kappa = -1.0$
- for double curvature case; max. moment at member ends.

• Other cases & APPROXIMATION

—  $\phi \frac{M_o}{M_y} = 1.0 \longrightarrow$  Eq. (21) Interaction eq<sup>n</sup>

The Eq. (21) was derived for linear moment gradient with loads. However this form holds for other loading cases (pg. 245 of book)

The interaction for  $\phi$  depends on  $\kappa$  &  $(F_r L)$ . It has to be developed for each problem. Therefore an approximation for  $\phi$  developed

$\phi = \dots \times \phi|_{\kappa=1}$  — (kind of a separation of variables)

and  $\phi$  depends on  $F_r L$

Now:  $\varphi|_{k=1} = \frac{\sqrt{2 - 2 \cos F_v L}}{\sin F_v L} \approx \frac{1}{1 - \frac{P}{P_E}}$

$\approx \frac{1}{1 - \frac{P}{P_E}}$

$\approx \frac{1}{1 - \left(\frac{F_v L}{\pi}\right)^2}$

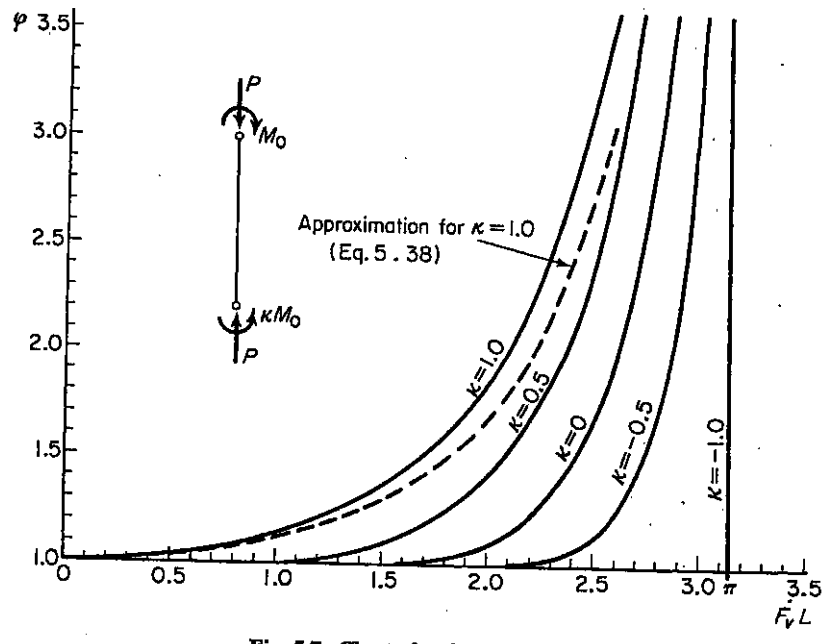


Fig. 5.7. Charts for determining  $\varphi$

And:  $C_{mm} = \sqrt{0.3 \kappa^2 + 0.4 \kappa + 0.3}$

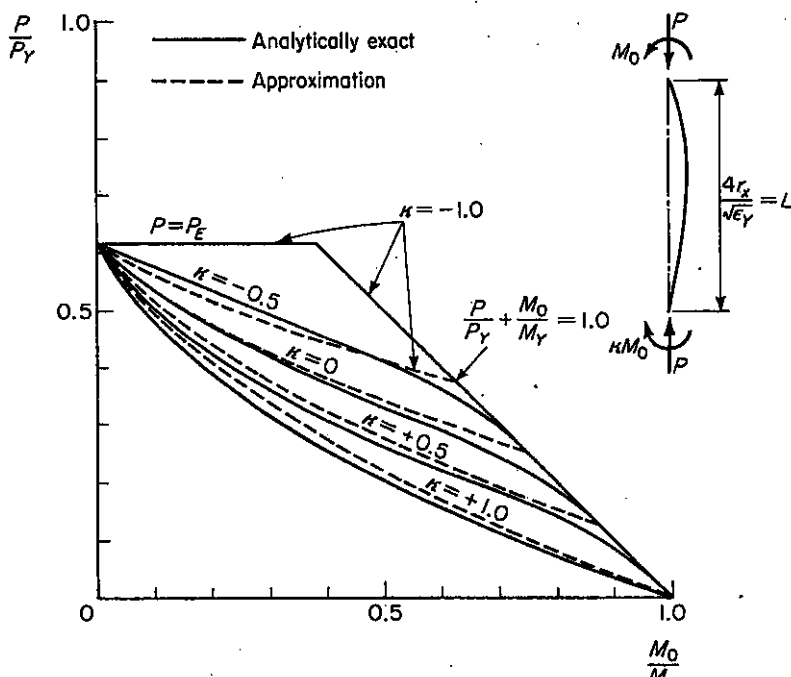
→ Massonet (Europe)

or  $C_m = 0.6 + 0.4 \kappa$

→ Austria (USA)

values are reasonable for  $-0.5 \leq \kappa \leq 1.0$





$$\therefore \frac{P}{P_Y} + \frac{C_m}{1 - \frac{P}{P_E}} \frac{M_0}{M_Y} = 1.0 \quad \longrightarrow \text{Eq. (22)}$$

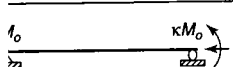
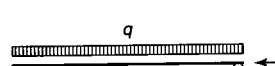

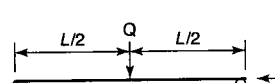
$$\text{where, } C_m = 0.6 + 0.4k \quad \longrightarrow \text{Eq. (23)}$$

The approximate Eq. (22) does not a/c for the case where  $M_{\max} = M_0$  at member end. Therefore need additional condition. Eq. (24) must also be satisfied.

$$\frac{P}{P_Y} + \frac{M_0}{M_Y} = 1.0 \quad \longrightarrow \text{Eq. (24)}$$

See above Figure.

## BLE 4.1 Moment Amplification Factors

Loading Case	Maximum First-order Moment	Moment Amplification Factor
	$M_o$	$\varphi = 1.0$ if $\kappa \leq \cos kL$ $\varphi = \frac{\sqrt{1 + \kappa^2 - 2\kappa \cos kL}}{\sin kL}$ if $\kappa \geq \cos kL$
	$M_o = \frac{qL^2}{8}$	$\varphi = \frac{8 \left(1 - \cos \frac{kL}{2}\right)}{(kL)^2 \cos \frac{kL}{2}}$
	$M_o = \frac{q_o L^2}{9\sqrt{3}}$	$\varphi = \frac{9\sqrt{3}}{(kL)^2} \left[ \frac{\sqrt{(kL)^2 - \sin^2 kL}}{kL \sin kL} - \frac{\arccos \frac{\sin kL}{kL}}{kL} \right]$
	$M_o = \frac{QL}{4}$	$\varphi = \frac{2 \tan \frac{kL}{2}}{kL}$

It is obvious that the four amplification factors do not differ from each other a great deal. For practical purposes, the four amplification factors are adequately represented by the much simpler formula

$$\varphi = \frac{1}{1 - P/P_E} \quad (4.7)$$

This formula appears to be intuitive, and it was probably so conceived in the first beam-column interaction equations used in design specifications, but it also has a mathematical significance, as discussed next.

Assume that the deflected shape of the beam-column is represented by the series of  $n$  sine shapes with amplitudes  $a_n$ , where  $n = 1, 2, 3, \dots$

$$v = \sum_1^n a_n \sin \frac{n\pi z}{L} \quad (4.8)$$

The first and second derivatives of  $v$  are equal to

$$v' = \sum_1^n \frac{n\pi a_n}{L} \cos \frac{n\pi z}{L}$$

$$-v'' = \sum_1^n \frac{n^2 \pi^2 a_n}{L^2} \sin \frac{n\pi z}{L}$$

The strain energy of bending is equal to

$$U = \frac{1}{2} \int_0^L EI (v'')^2 dz = \frac{EI \pi^4}{2L^4} \cdot \frac{L}{2} \sum_1^n a_n^2 n^4$$

because

$$\int_0^L \sin^2 \frac{n\pi z}{L} dz = \frac{L}{2}$$

$$\int_0^L \sin \frac{n\pi z}{L} \cdot \sin \frac{m\pi z}{L} dz = 0, n \neq m$$

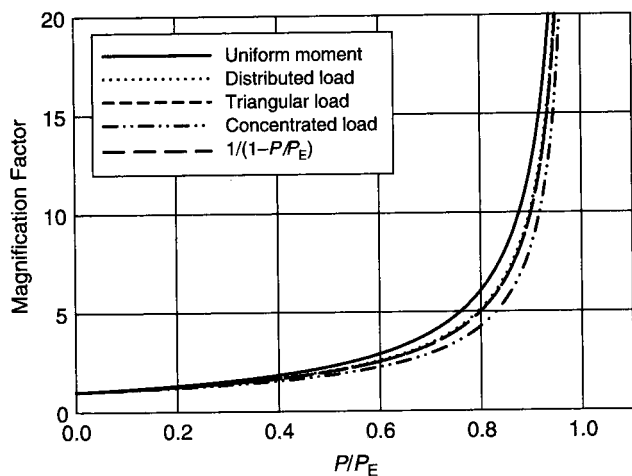


Fig. 4.8 Relationship between axial load and moment magnifiers for various loading conditions.

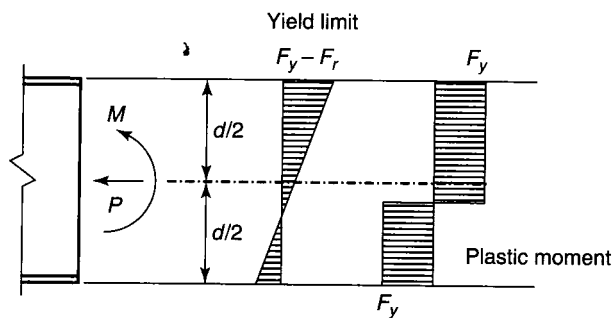


Fig. 4.34 Strength limits of the cross-section.

For a rectangular cross-section, the plastic moment has been derived already in Chapter 3 as the limiting case where the curvature approaches very large values (see Figure 3.18). It will be rederived here again based on equilibrium of the stress blocks. The location of  $P$  and  $M_{pc}$ , the cross-section and the stress distribution for the plastic moment condition are given in Figure 4.35.

The total stress distribution can be separated into the contribution due to the axial force and due to the bending moment.

$$\text{Yield load: } P_y = b d F_y \quad (4.42)$$

$$\text{Plastic moment when } P = 0: M_p = \frac{b d^2 F_y}{4} \quad (4.43)$$

$$\text{Axial stress equilibrium: } P = (2y_p - d)bF_y$$

$$\frac{P}{b d F_y} = \frac{P}{P_y} = \frac{2y_p}{d} - 1$$

$$\frac{y_p}{d} = \frac{1}{2} \left( 1 + \frac{P}{P_y} \right)$$

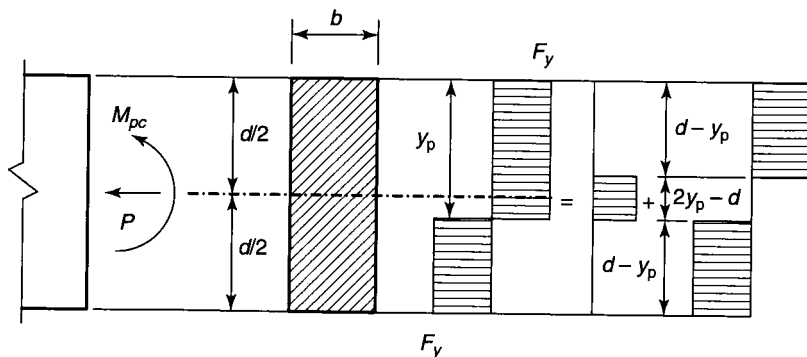


Fig. 4.35 Plastic moment of a rectangular cross-section.

$$\text{Moment equilibrium: } M_{pc} = (d - y_p)bF_y \times \left( d - \frac{2(d - y_p)}{2} \right)$$

$$M_{pc} = (d - y_p)y_p \times bF_y = \frac{b d^2 F_y}{4} \left( 1 - \frac{P}{P_y} \right) \left( 1 + \frac{P}{P_y} \right)$$

$$\frac{M_{pc}}{M_p} = 1 - \left( \frac{P}{P_y} \right)^2 \quad (4.44)$$

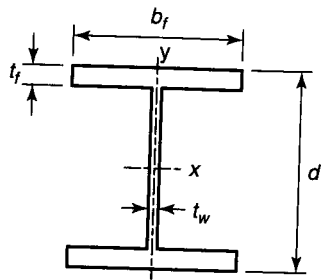
Equation 4.44 is the plastic moment in the presence of axial force for a rectangular cross-section. The formulas for  $M_{pc}$  for other cross-sections are derived in a similar manner, but they are more complicated, of course, depending on the cross-sectional geometry. The equations for the plastic moments for  $x$ -axis and  $y$ -axis bending of wide-flange shapes are in Table 4.4. Simpler approximate formulas are also given in the table (*Plastic Design in Steel* ASCE 1971). These approximate equations are compared with the analytically exact formulas in Figure 4.36, where the axial ratio is the ordinate and the bending ratio is the abscissa. The exact formulas were calculated for the geometry of a W14  $\times$  99 rolled wide-flange shape. The curves for the approximate formulas are seen to be close enough for practical purposes.

The approximate formula for a solid circular cross-section of radius  $R$  is given as equation 4.45. This is a very good approximation of a complicated exact equation.

$$\frac{M_{pc}}{M_p} = 1 + 0.08 \frac{P}{P_y} - 1.08 \left( \frac{P}{P_y} \right)^2; \quad P_y = \pi R^2 F_y; \quad M_p = \frac{4R^3 F_y}{3} \quad (4.45)$$

The curves from the analytically exact equations are shown in Figure 4.37, starting with the top dashed line, of a W14  $\times$  99 wide-flange section bent about the minor axis, a solid circular section, a rectangular section, and a W14  $\times$  99 wide-flange section bent about the major axis, respectively. The solid line represents the lower-bound interaction equation that is the basis of the AISC Specification for the design of beam-columns. As can be seen, the AISC equation closely replicates the  $x$ -axis interaction strength of the wide-flange shape. Since the AISC equation is a lower bound to the most frequent practical situation, it was adopted for use in the design standard. It should be realized, however, that for other shapes it can be very conservative. Equation 4.46 is the AISC basic interaction equation.

TABLE 4.4 Plastic Moments for Wide-flange Shapes



$$M_{px} = Z_x F_y$$

$$M_{py} = Z_y F_y$$

Bending about x-axis

$$\text{for } 0 \leq \frac{P}{P_y} \leq \frac{t_w(d - 2t_f)}{A}$$

$$\frac{M_{pcx}}{M_{px}} = 1 - \frac{A^2 \left(\frac{P}{P_y}\right)^2}{4t_w Z_x}$$

$$\text{for } \frac{t_w(d - 2t_f)}{A} \leq \frac{P}{P_y} \leq 1$$

$$\frac{M_{pcx}}{M_{py}} = \frac{A \left(1 - \frac{P}{P_y}\right)}{2Z_x} \left[ d - \frac{A \left(1 - \frac{P}{P_y}\right)}{2b_f} \right]$$

Approximation:

$$\frac{M_{pcx}}{M_{px}} = 1.18 \left(1 - \frac{P}{P_y}\right) \leq 1.0$$

Bending about y-axis

$$\text{for } 0 \leq \frac{P}{P_y} \leq \frac{t_w d}{A}$$

$$\frac{M_{pc}}{M_p} = 1 - \frac{A^2 \left(\frac{P}{P_y}\right)^2}{4dZ_y}$$

$$\text{for } \frac{t_w d}{A} \leq \frac{P}{P_y} \leq 1$$

$$\frac{M_{pc}}{M_p} = \frac{A^2 \left(1 - \frac{P}{P_y}\right)}{8t_f Z_y} \left[ \frac{4b_f t_f}{A} - \left(1 - \frac{P}{P_y}\right) \right]$$

Approximation:

$$\frac{M_{pcy}}{M_{py}} = 1.19 \left[ 1 - \left(\frac{P}{P_y}\right)^2 \right] \leq 1.0$$

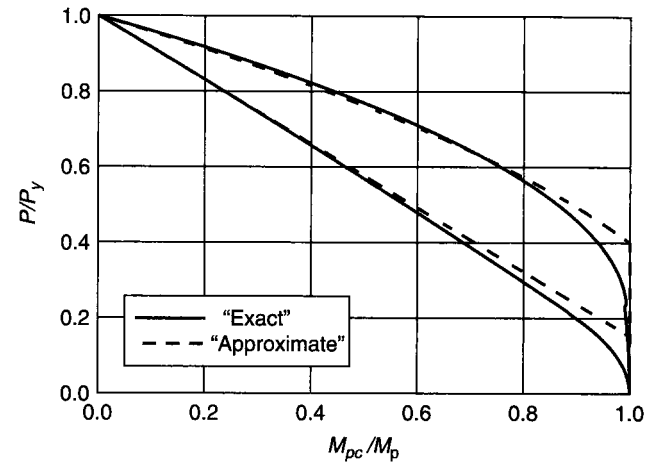


Fig. 4.36 Exact and approximate  $M$ - $P$  relations for  $x$ -axis bending (lower curves) and  $y$ -axis bending (upper curves) of a  $W14 \times 99$  wide-flange section.

$$\frac{1}{2} \frac{P}{P_y} + \frac{M_{pc}}{M_p} = 1 \quad \text{if } \frac{P}{P_y} \leq 0.2$$

$$\frac{P}{P_y} + \frac{8M_{pc}}{9M_p} = 1 \quad \text{if } \frac{P}{P_y} \geq 0.2 \tag{4.46}$$

The previous discussion above considered the plastic strength of a cross-section that is subjected to an axial force at its geometric centroid and to a

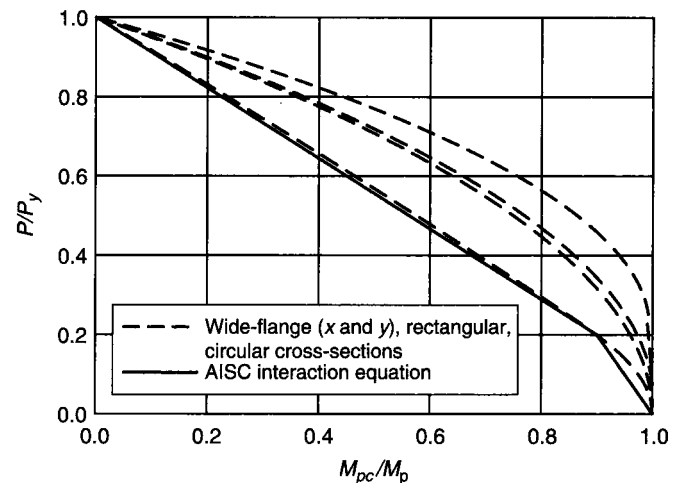


Fig. 4.37 Comparison of cross-section interaction curves with AISC interaction equation.

### 4.2.3 Elastic Lateral-Torsional Buckling behavior

Most general equations were (8) & (11)

$$EI_y u^{iv} + Pu'' + M_0 \left[ 1 - \frac{z}{L} (1-\kappa) \right] \phi'' - \frac{2M_0}{L} (1-\kappa) \phi' + P y_0 \phi'' = 0 \quad \longrightarrow (8)$$

$$EI_\omega \phi^{iv} - [GK_T - P\bar{r}_0^2 + M_x \beta_x] \phi'' + M_0 \beta_x \phi' \left( \frac{1-\kappa}{L} \right) + M_x u'' + P y_0 u'' = 0 \quad \longrightarrow (11)$$

The phenomenon will be identical to the lateral-torsional buckling of beams & columns.

The critical combination of loads producing it are the max. practical load that can be sustained by the member.

Eq. (8) & (11) can be solved for singly symmetric sections ( $\kappa_0 = 1$  & unequal end moments ( $\kappa \neq 1$ ) by numerical methods.

For doubly symmetric sections ( $y_0 = \beta_x = 0$ ) the d.e. become

$$EI_y u^{iv} + Pu'' + M_0 \left[ 1 - \frac{z}{L} (1-\kappa) \right] \phi'' - \frac{2M_0}{L} (1-\kappa) \phi' = 0 \quad \longrightarrow (25)$$

$$EI_\omega \phi^{iv} - [GK_T - P\bar{r}_0^2] \phi'' + M_0 \left[ 1 - \frac{z}{L} (1-\kappa) \right] u'' = 0 \quad \longrightarrow (26)$$

Eq. (25) & (26) are best solved by numerical or energy methods. Salvadori used the Rayleigh-Ritz method & presented the results.

• Consider Eq. (25) & (26) with  $\kappa = 1.0$

$$\therefore EI_y u'''' + Pu'' + \frac{7}{8} M_0 \phi'' = 0$$

$$EI_\omega \phi'''' - (GK_T - P\bar{r}_0^2) \phi'' + M_0 u'' = 0$$

Assume s.s. boundary conditions

$u(0) = 0$	$u(L) = 0$
$u''(0) = 0$	$u''(L) = 0$
$\phi(0) = 0$	$\phi(L) = 0$
$\phi''(0) = 0$	$\phi''(L) = 0$

$$\therefore u = C_1 \sin \frac{\pi z}{L} \quad \& \quad \phi = C_2 \sin \frac{\pi z}{L}$$

$$\therefore \left[ \left( \frac{\pi^2 EI_y}{L^2} - P \right) C_1 - M_0 C_2 \right] \times \frac{\pi^2}{L^2} \sin \frac{\pi z}{L} = 0$$

$$\& \left[ -M_0 C_1 + \left( \frac{\pi^2 EI_\omega}{L^2} + GK_T - P\bar{r}_0^2 \right) C_2 \right] \times \frac{\pi^2}{L^2} \sin \frac{\pi z}{L} = 0$$

$$\therefore \begin{bmatrix} \frac{\pi^2 EI_y}{L^2} - P & -M_0 \\ -M_0 & \frac{\pi^2 EI_\omega}{L^2} - P\bar{r}_0^2 + GK_T \end{bmatrix} \begin{Bmatrix} C_1 \\ C_2 \end{Bmatrix} = 0$$

$$\therefore (\det) = 0$$

$$\therefore (P_y - P) (\bar{r}_o^2 P_z - P \bar{r}_o^2) - M_o^2 = 0$$

$$\therefore M_o = \sqrt{(P_y - P) (P_z - P) \bar{r}_o^2} \quad \longrightarrow (27)$$

where,  $P_y = \frac{\pi^2 E I_y}{L^2}$  and  $P_z = \frac{\pi^2 E I_w}{L^2} + G K_T$   
 $\bar{r}_o^2$

- Eq. (27) gives the P-Mo<sub>cr</sub> relationship for a doubly symmetric elastic member with  $\eta = 1.0$

$$\therefore M_o)_{cr} = \sqrt{(P_y - P) (P_z - P) \times \frac{(I_x + I_y)}{A}}$$

- Consider the member with  $x_o = 0$ ;  $y_o \neq 0$ ;  $\beta_x \neq 0$  (singly symmetric) with  $\eta = 1$

Then. 
$$\begin{vmatrix} P_y - P & -(M_o + P y_o) \\ -(M_o + P y_o) & (\bar{r}_o^2 P_z - P \bar{r}_o^2 + M_o \beta_x) \end{vmatrix} = 0$$

$$\therefore (P_y - P) (\bar{r}_o^2 P_z - P \bar{r}_o^2 + M_o \beta_x) = (M_o + P y_o)^2 \quad \longrightarrow (28)$$

Eq. (28) gives the critical relation between P-Mo leading to elastic lateral-torsional buckling.

• Effect of lateral-torsional buckling on W8x31 for  
 $\frac{L}{r_x} \times \sqrt{E_r} = 1.99$  &  $\frac{L}{r_x} \times \sqrt{E_r} = 3.98$

- Lateral-torsional buckling controls everywhere for  
 $\frac{L}{r_x} \sqrt{E_r} = 3.98$

- Lateral-torsional buckling governs for small portion of  
 $\frac{L}{r_x} \sqrt{E_r} = 1.99$

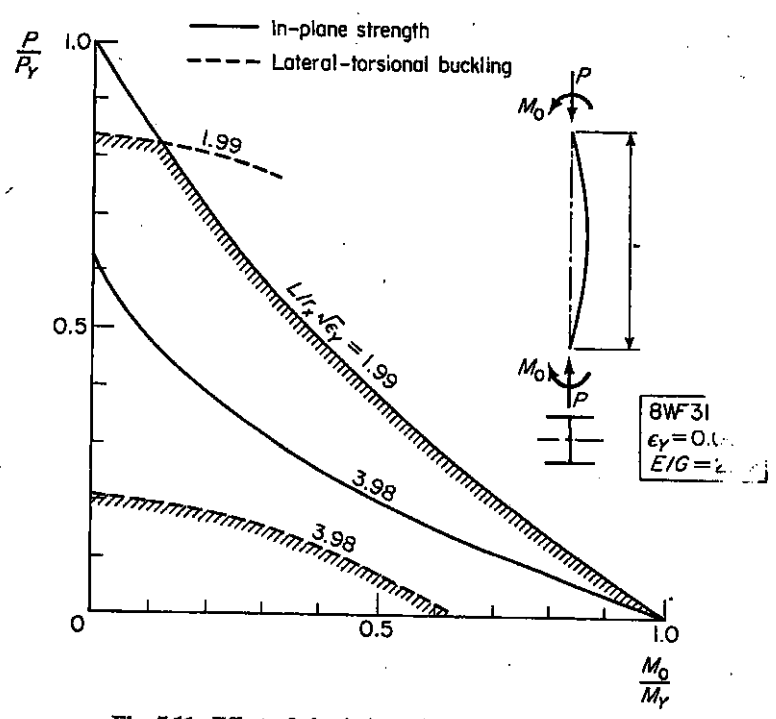


Fig. 5.11. Effect of elastic lateral-torsional buckling



- Another way of illustrating lateral-torsional buckling

$$\frac{M_0}{M_y} \text{ vs. } \frac{L}{r_x}$$

- The curve for elastic strength from  $\frac{P}{P_y} + \phi \frac{M_0}{M_y} = 1.0$
- The curve for elastic LTB for N 8x31 & N 27x94 are also shown.

For efficient use of beam-columns, bracing must be provided between member ends so that LTB strength  $>$  in-plane str.

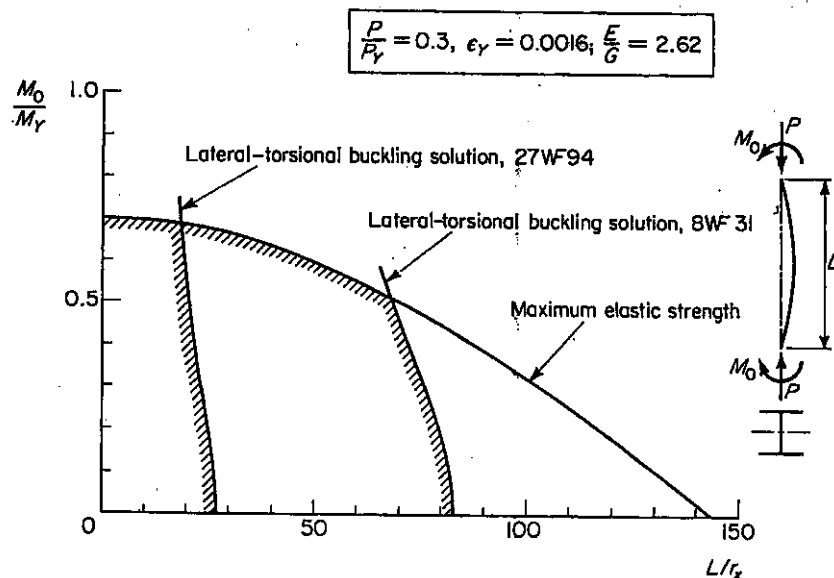


Fig. 5.12. Cross-section effect on elastic lateral-torsional buckling

- Boundary Condition effects see pg. 252 of Galambos